2014-01

A novel ozone gas sensor based on one-dimensional (1D) -Ag2WO4 nanostructures

Nanoscale,Cambridge : Royal Society of Chemistry - RSC, v. 6, p. 4058-4062, Jan. 2014
http://www.producao.usp.br/handle/BDPI/50206

Nanoscale

COMMUNICATION

View Article Online
View Journal | View Issue

Cite this: *Nanoscale*, 2014, **6**, 4058

A novel ozone gas sensor based on one-dimensional (1D) α-Ag_2WO_4 nanostructures†

Luís F. da Silva,*[a] Ariadne C. Catto,[b] Waldir Avansi, Jr.,[c] Laécio S. Cavalcante,[d] Juan Andrés,[e] Khalifa Aguir,[f] Valmor R. Mastelaro[b] and Elson Longo[a]

Received 1st November 2013
Accepted 28th January 2014

DOI: 10.1039/c3nr05837a

www.rsc.org/nanoscale

This paper reports on a new ozone gas sensor based on α-Ag_2WO_4 nanorod-like structures. Electrical resistance measurements proved the efficiency of α-Ag_2WO_4 nanorods, which rendered good sensitivity even for a low ozone concentration (80 ppb), a fast response and a short recovery time at 300 °C, demonstrating great potential for a variety of applications.

Metal semiconducting oxides have drawn the interest of many researchers due to their wide range of applications, especially as gas sensing materials.[1–5] Among them, one-dimensional (1-D) semiconductor nanostructures have been proposed as very interesting materials, especially as gas sensor devices.[6–12] It is well known that several technological applications of nanostructured materials are directly related to the morphology, particle size, crystalline phase and activity of specific crystalline planes strictly dependent on synthesis methods.[4,13–15] In particular, the relationship between morphology and gas sensing properties has been well established.[4,16,17]

Tungsten-based oxides are an important class of materials that display wide potential functional properties,[18–20] specifically the silver tungstate (Ag_2WO_4) compound, which can exhibit three different structures: α-orthorhombic, β-hexagonal, and γ-cubic.[21–25] Recently, our research group reported a detailed study of the synthesis, structural and optical properties of hexagonal nanorod-like elongated α-Ag_2WO_4 nanocrystals obtained by different methods.[26–28]

Ozone (O_3) is an oxidizing gas used in many technological applications in different areas, such as the food industry, drinking-water treatment, medicine, microelectronic cleaning processes, and others.[29,34–39] For example, ozone has been employed as a powerful drinking-water disinfectant and oxidant.[34,35,40] On the other hand, when the ozone level in an atmosphere exceeds a certain threshold value, the exposure to this gas becomes hazardous to human health and can cause serious health problems (*e.g.* headache, burning eyes, respiratory irritation and lung damage).[34,41] The European Guidelines (2002/3/EG) recommend avoiding exposure to ozone levels above 120 ppb.[41] Such arguments support the requirement for the determination and continuous monitoring of ozone levels.[3,29,41]

Gas sensing properties are evaluated in terms of operating temperature, sensitivity, response time, recovery time and stability.[29–33] SnO_2, In_2O_3 and WO_3 compounds have been considered the most promising ozone gas sensors.[29–33]

To the best of our knowledge, to date the gas sensing properties of α-Ag_2WO_4 nanocrystals have never been evaluated.

Here, we report the sensing properties of 1-D α-Ag_2WO_4 nanorod-like structures obtained by the microwave-assisted hydrothermal (MAH) method.[42–46] Because of such properties, nanorods are potential candidates for practical applications as ozone gas sensors.

The crystalline phase of the as-obtained α-Ag_2WO_4 sample was analyzed by X-ray diffraction measurement and all reflections were indexed to an orthorhombic structure with a *Pn2n* space group (ICSD file no. 4165) with no secondary phases (see Fig. S1, ESI†).

The FE-SEM and TEM images in Fig. 1 show that the α-Ag_2WO_4 crystals exhibit a one-dimensional (1D) and uniform morphology composed of 100 nm wide nanorods. The one-dimensional nature observed for the as-prepared nanostructures is related to the preferential growth in the [001]

[a]*LIEC, Instituto de Química, Universidade Estadual Paulista, P.O. Box 355, 14800-900 Araraquara, SP, Brazil. E-mail: lfsilva83@gmail.com; Tel: +55 16 33016643*
[b]*Instituto de Física de São Carlos, Universidade de São Paulo, Avenida Trabalhador São-carlense, 400, 13566-590 São Carlos, SP, Brazil. Tel: +55 16 33739828*
[c]*Departamento de Física, Universidade Federal de São Carlos, Rodovia Washington Luiz, km 235, 13565-905 São Carlos, SP, Brazil*
[d]*Departamento de Química, Universidade Estadual do Piauí, 64002-150 Teresina, PI, Brazil*
[e]*Departamento Química-Física y Analítica, Universitat Jaume I, Campus de Riu Sec, Castelló E-12080, Spain*
[f]*Aix Marseille Université, CNRS IM2NP (UMR 7334), FS St Jérôme S152, Marseille, 13397, France*

† Electronic supplementary information (ESI) available: The X-ray diffraction pattern and ozone gas sensor response at an operating temperature of 300 °C and 350 °C. See DOI: 10.1039/c3nr05837a

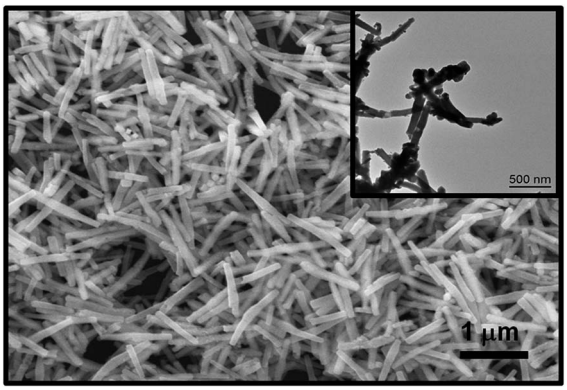

Fig. 1 FE-SEM image of the α-Ag_2WO_4 nanorods. The inset shows a TEM image of the nanorods.

direction.[27,28] Additionally, the α-Ag_2WO_4 nanorods exhibit other nanoparticles on their surface. Recently, we reported the real-time *in situ* observation of the silver metallic (Ag) growth process from the unstable α-Ag_2WO_4 nanorods submitted to electron irradiation from a transmission electron microscope.[27,28] Nevertheless, we must emphasize that the α-Ag_2WO_4 nanorods used in the ozone sensor measurements were not exposed to electron irradiation, and consequently, Ag nanoparticles are not present on the α-Ag_2WO_4 nanorods' surface.

The resistance response of the α-Ag_2WO_4 nanorods was studied at an operating temperature of 300 °C under the exposure of 500 ppb of ozone gas at different times (15, 30 and 60 s) and the results are depicted in Fig. 2. The electrical resistance response is typical of an n-type semiconductor material exposed to oxidizing gases. The oxygen species (O_2^- and O^-) chemisorbed onto the semiconductor surface decrease the conductivity of the sensor device due to the lower concentration of free electrons in the conduction band.[29,33] It is noteworthy that the α-Ag_2WO_4 nanorods display good sensitivity, a fast response as well as a short recovery time (Table 1).

As can be seen in Fig. 2, the sample also exhibits good sensitivity to the different exposure times as well as total reversibility and good stability of the base line.

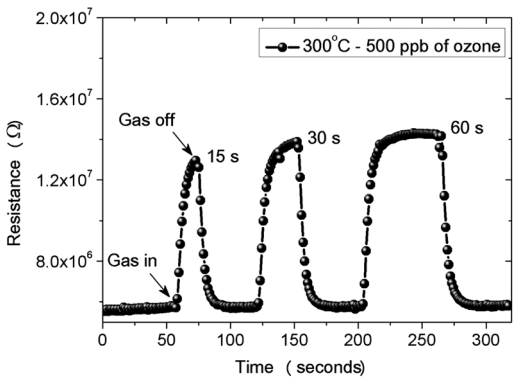

Fig. 2 Ozone gas sensing response for α-Ag_2WO_4 nanorods upon exposure to differing times at an operating temperature of 300 °C. Arrows indicate when the ozone gas flow was turned on and off.

Table 1 Comparison of the parameters of ozone gas sensing properties of the α-Ag_2WO_4 sample and WO_3-, In_2O_3-, and SnO_2-based chemiresistors

Sensor	Operating temp. (°C)	Ozone level (ppb)	Response time (s)	Recovery time (s)	Reference
WO_3	250	80	1	60	33
In_2O_3	300	100	60	6000	31
SnO_2	250	1000	2	1000	29
Ag_2WO_4	300	930	6	16	This study
Ag_2WO_4	300	500	7	14	This study
Ag_2WO_4	300	80	7	13	This study

Fig. 3(a) shows the ozone gas sensing performance of α-Ag_2WO_4 nanorods at different operating temperatures (300 °C and 350 °C) and different ozone concentrations. For both operating temperatures, the sensitivity increases with ozone concentration and greater sensitivity is observed at 300 °C, considered the best operating temperature. The ozone gas responses of α-Ag_2WO_4 nanorods at 300 °C and 350 °C upon exposure to different gas concentrations are displayed in Fig. S2 and S3 (ESI†).

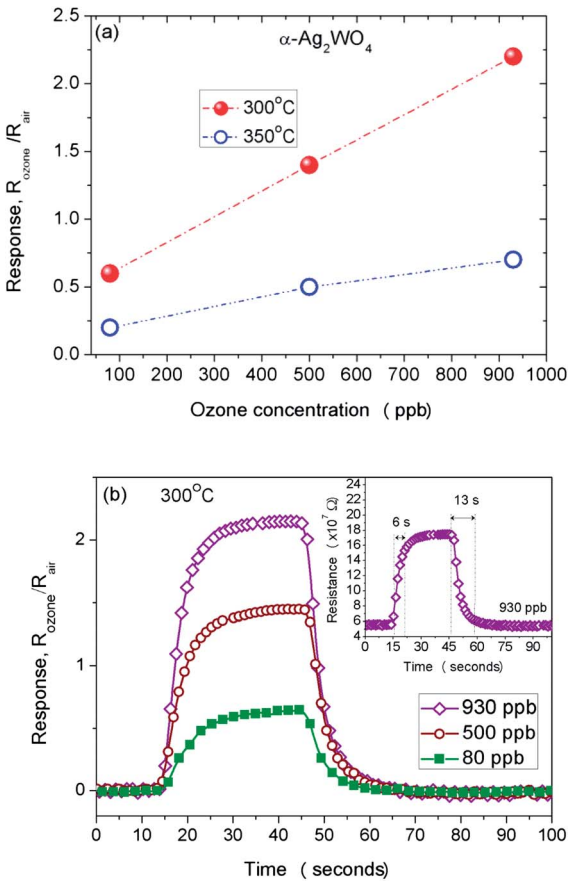

Fig. 3 Dependence of response on the ozone concentration of α-Ag_2WO_4 nanorods (a) at an operating temperature of 300 °C and 350 °C. (b) Ozone gas sensor response at 300 °C. The inset shows the response and recovery time for 930 ppb of ozone.

The ozone sensitivity of α-Ag_2WO_4 nanorods operating at 300 °C and exposed to a range of ozone concentration from 80 to 930 ppb was also evaluated and the results are shown in Fig. 3(b). The α-Ag_2WO_4 nanorod-based sensor displayed good sensitivity and no evidence of saturation in the concentration range evaluated. As can be seen in Table 1, even at a low concentration (80 ppb), they exhibit a fast response time of 7 s and a short recovery time of 13 s, similar to the results for high concentrations of ozone.

For comparison, Table 1 also shows the results reported for WO_3-, In_2O_3- and SnO_2-based ozone gas sensors.[29,31,33] An analysis of the results has revealed that the operating temperature of the α-Ag_2WO_4-based sensor is close to that of WO_3, In_2O_3 and SnO_2 materials and the response time is slightly longer than those of WO_3- and SnO_2-based sensors, but significantly shorter than those of In_2O_3-based sensors. On the other hand, the recovery time of the α-Ag_2WO_4-based sensor is shorter than those of WO_3-, In_2O_3- and SnO_2-based sensors.

We can propose two effects of O_3 adsorption in the α-Ag_2WO_4 sample. The α-Ag_2WO_4 crystals have an orthorhombic structure and distorted $[WO_6]$ clusters with an octahedral configuration, therefore, the α-Ag_2WO_4 orthorhombic structure has four different types of coordination for the Ag^+ ion and six possible configurations for the $[AgO_x]$, $x = 2$, 4, 6 or 7 clusters. For the tetrahedral $[AgO_4]$ and deltahedral $[AgO_7]$ clusters, there are two possible configurations, as shown by the different bonds, distances and angles.[26–28] The first effect is intrinsic to that of the sample and the second is a consequence of the surface and interface complex cluster defects which produce extrinsic defects. Before the adsorption of O_3, the short and medium range order structural defects generate non-homogeneous charge distribution in the cell. After the O_3 adsorption, the configuration charges and distorted excited clusters are formed, allowing electrons to become trapped (O_3'). Therefore the gas sensing mechanism can be described according to the following equations:

The first effect,

$$[WO_6]^{\times} - [WO_5V_O^{\times}] \rightarrow [WO_6]' - [WO_5V_O^{\cdot}] \quad (1)$$

$$[WO_6]' - [WO_5V_O^{\cdot}] + O_3 \rightarrow [WO_6]' - [WO_5V_O^{\cdot\cdot}]\ldots O_3'(\text{ads}) \quad (2)$$

$$[WO_6]' - [WO_5V_O^{\cdot\cdot}]\ldots O_3' \rightarrow [WO_6]' - [WO_5V_O^{\cdot}] + O^* + O_2\ (\text{des}) \quad (3)$$

The second effect,

$$[WO_6]_O^{\times} - [WO_5]_d^{\times} \rightarrow [WO_6]_O' - [WO_5]_d^{\cdot} \quad (4)$$

$$[WO_6]_O' - [WO_5]_d^{\cdot} + O_3 \rightarrow [WO_6]_O^{\times} - [WO_5]_d^{\cdot}\ldots\ O_3'\ (\text{ads}) \quad (5)$$

$$[WO_6]_O^{\times} - [WO_5]_d^{\cdot}\ldots O_3' \rightarrow [WO_6]_O^{\times} - [WO_5]_d^{\times} + O^* + O_2\ (\text{des}) \quad (6)$$

$$[AgO_x]^{\times} - [AgO_{x-1}V_O^{\times}] \rightarrow [AgO_x]' - [AgO_{x-1}V_O^{\cdot}] \quad (7)$$

$$[AgO_x]' - [AgO_{x-1}V_O^{\cdot}] + O_3 \rightarrow [AgO_x]' - [AgO_{x-1}V_O^{\cdot\cdot}]\ldots O_3' \quad (8)$$

$$[AgO_x]' - [AgO_{x-1}V_O^{\cdot\cdot}]\ldots O_3' \rightarrow [AgO_x] - [AgO_{x-1}V_O^{\cdot}] + O^* + O_2\ (\text{des}) \quad (9)$$

Conclusions

The α-Ag_2WO_4 nanorod-like structures obtained *via* the MAH route were evaluated as promising ozone sensors. They have shown great potential as novel ozone gas sensors and displayed good sensitivity to low ozone concentrations as well as good stability, a fast response and a short recovery time.

Experimental section

Preparation of α-Ag_2WO_4 nanorods

α-Ag_2WO_4 powder was prepared at 160 °C for 1 h with 1 g of PVP40 ($(C_6H_9NO)_n$; 99%) by the MAH method. All reagents were obtained from Aldrich company. The typical α-Ag_2WO_4 sample synthesis procedure is described as follows: 1 mM of $Na_2WO_4 \cdot 2H_2O$ (99.5%) and 2 mM of $AgNO_3$ (99.8%) were separately dissolved with deionized water contained in two plastic tubes of 50 mL each. Before the dissolution of the salts, 0.5 g of polymer surfactant (PVP40) was dissolved in both tubes. 100 mL of the suspension were transferred to a Teflon vessel autoclave. The Teflon reactor was then sealed, placed inside an adapted domestic microwave system and processed for 1 h at 160 °C. The resulting suspension was washed with deionized water several times for the removal of the remaining Na^+ ions and organic compounds. Finally, a light beige powdered precipitate was collected and dried with acetone for 6 h at room temperature.

Structural and morphological characterization

The sample was structurally characterized by X-ray diffraction (XRD) using CuKα radiation (Rigaku diffractometer, model D/Max-2500PC) in a 2θ range from 10° to 70° with a step of 0.02° at a scanning speed of 2° min^{-1}. The morphology of the as-obtained sample was studied by transmission electron microscopy (TEM) on a JEM 2010 URP operating at 200 kV and by field emission scanning electron microscopy (FE-SEM) on a Zeiss Supra35 operating at 5 kV.

Gas sensor preparation

The α-Ag_2WO_4 powders were dispersed in isopropyl alcohol by an ultrasonic cleaner for 30 minutes and the suspension was then dripped onto a SiO_2/Si substrate containing 100 nm thick Pt electrodes separated by a distance of 50 μm. The sample was heat-treated for 2 hours at 500 °C in an electric furnace in air.

Ozone gas sensor measurements

The sensor sample was inserted into a test chamber for the control of the temperature under different ozone concentrations. The ozone gas was formed by oxidation of oxygen molecules of dry air (8.3 $cm^3\ s^{-1}$) with a calibrated pen-ray UV lamp (UVP, model P/N 90-0004-01) and provided ozone

concentrations from 80 to 930 ppb. The dry air containing ozone was blown directly onto the sensor placed on a heated holder. The dc voltage applied was 1 V while the electrical resistance was measured using a Keithley (model 6514) electrometer. The response (S) was defined as $S = R_{ozone}/R_{air}$, where R_{ozone} and R_{air} are the electric resistances of the sensor exposed to ozone gas and dry air, respectively.

The response time of the sensor was defined as the time required for a change in the sample's electrical resistance to reach 90% of the initial value when exposed to ozone gas. Similarly, the recovery time was defined as the time required for the electrical resistance of the sensor to reach 90% of the initial value after the ozone gas has been turned off.

Acknowledgements

The authors would like to acknowledge Rorivaldo Camargo for operating the FE-SEM equipment. They are also grateful for the financial support provided by the Brazilian research funding institution CNPq and FAPESP (under grants no. 2013/07296-2 and 2013/09573-3). This research was partially developed at the Brazilian Nanotechnology National Laboratory (LNNano). J. Andrés also acknowledges the support of Generalitat Valenciana under project Prometeo/2009/053, Ministerio de Ciencia e Innovación under project CTQ2009-14541-C02, Programa de Cooperación Científica con Iberoamerica (Brasil) and Ministerio de Educación (PHB2009-0065-PC).

Notes and references

1 X. Chen, C. K. Y. Wong, C. A. Yuan and G. Zhang, *Sens. Actuators, B*, 2013, **177**, 178–195.
2 E. Comini, C. Baratto, I. Concina, G. Faglia, M. Falasconi, M. Ferroni, V. Galstyan, E. Gobbi, A. Ponzoni, A. Vomiero, D. Zappa, V. Sberveglieri and G. Sberveglieri, *Sens. Actuators, B*, 2013, **179**, 3–20.
3 V. R. Mastelaro, S. C. Zílio, L. F. da Silva, P. I. Pelissari, M. I. B. Bernardi, J. Guerin and K. Aguir, *Sens. Actuators, B*, 2013, **181**, 919–924.
4 D. P. Volanti, A. A. Felix, M. O. Orlandi, G. Whitfield, D. J. Yang, E. Longo, H. L. Tuller and J. A. Varela, *Adv. Funct. Mater.*, 2013, **23**, 1759–1766.
5 E. Rossinyol, J. Arbiol, F. Peiró, A. Cornet, J. R. Morante, B. Tian, T. Bo and D. Zhao, *Sens. Actuators, B*, 2005, **109**, 57–63.
6 E. Comini, *Anal. Chim. Acta*, 2006, **568**, 28–40.
7 M. Sarikaya, C. Tamerler, D. T. Schwartz and F. Baneyx, *Annu. Rev. Mater. Res.*, 2004, **34**, 373–408.
8 A. Kolmakov and M. Moskovits, *Annu. Rev. Mater. Res.*, 2004, **34**, 151–180.
9 M. E. Franke, T. J. Koplin and U. Simon, *Small*, 2006, **2**, 301.
10 Y. Cui, Q. Q. Wei, H. K. Park and C. M. Lieber, *Science*, 2001, **293**, 1289–1292.
11 G. Shen, P.-C. Chen, K. Ryu and C. Zhou, *J. Mater. Chem.*, 2009, **19**, 828–839.
12 K. J. Choi and H. W. Jang, *Sensors*, 2010, **10**, 4083–4099.
13 H. Mourao, A. R. Malagutti and C. Ribeiro, *Appl. Catal., A*, 2010, **382**, 284–292.
14 G. Korotcenkov, *Mater. Sci. Eng., R*, 2008, **61**, 1–39.
15 L. F. da Silva, W. Avansi, M. L. Moreira, A. Mesquita, L. J. Q. Maia, J. Andres, E. Longo and V. R. Mastelaro, *J. Nanomater.*, 2012, **2012**, 890397.
16 M. R. Alenezi, S. J. Henley, N. G. Emerson and S. R. Silva, *Nanoscale*, 2014, **6**, 235–247.
17 M. M. Arafat, B. Dinan, S. A. Akbar and A. S. M. A. Haseeb, *Sensors*, 2012, **12**, 7207–7258.
18 S.-H. Yu, B. Liu, M.-S. Mo, J.-H. Huang, X.-M. Liu and Y.-T. Qian, *Adv. Funct. Mater.*, 2003, **13**, 639–647.
19 P. Hu and Y. Cao, *Dalton Trans.*, 2012, **41**, 8908–8912.
20 S.-H. Yu, M. Antonietti, H. Cölfen and M. Giersig, *Angew. Chem., Int. Ed.*, 2002, **41**, 2356–2360.
21 A. J. Vandenberg and C. A. H. Juffermans, *J. Appl. Crystallogr.*, 1982, **15**, 114–116.
22 Q. P. Wang, X. X. Guo, W. H. Wu and S. X. Liu, in *Mater. Des., Pts 1–3*, ed. X. M. Sang, P. C. Wang, L. Ai, Y. G. Li and J. L. Bu, 2011, vol. 284–286, pp. 1321–1325.
23 R. R. Kharade, S. S. Mali, S. P. Patil, K. R. Patil, M. G. Gang, P. S. Patil, J. H. Kim and P. N. Bhosale, *Electrochim. Acta*, 2013, **102**, 358–368.
24 L. Pan, L. Li and Y. H. Chen, *J. Sol-Gel Sci. Technol.*, 2013, **66**, 330–336.
25 J. Tang and J. Ye, *J. Mater. Chem.*, 2005, **15**, 4246–4251.
26 L. S. Cavalcante, M. A. P. Almeida, W. Avansi, R. L. Tranquilin, E. Longo, N. C. Batista, V. R. Mastelaro and M. S. Li, *Inorg. Chem.*, 2012, **51**, 10675–10687.
27 E. Longo, L. S. Cavalcante, D. P. Volanti, A. F. Gouveia, V. M. Longo, J. A. Varela, M. O. Orlandi and J. Andres, *Sci. Rep.*, 2013, **3**, 1676.
28 E. Longo, D. P. Volanti, V. M. Longo, L. Gracia, I. C. Nogueira, M. A. P. Almeida, A. N. Pinheiro, M. M. Ferrer, L. S. Cavalcante and J. Andres, *J. Phys. Chem. C*, 2014, **118**, 1229–1239.
29 G. Korotcenkov and B. K. Cho, *Sens. Actuators, B*, 2012, **161**, 28–44.
30 G. Korotcenkov, I. Blinov, M. Ivanov and J. R. Stetter, *Sens. Actuators, B*, 2007, **120**, 679–686.
31 M. Epifani, S. Capone, R. Rella, P. Siciliano, L. Vasanelli, G. Faglia, P. Nelli and G. Sberveglieri, *J. Sol-Gel Sci. Technol.*, 2003, **26**, 741–744.
32 K. Aguir, C. Lemire and D. B. B. Lollman, *Sens. Actuators, B*, 2002, **84**, 1–5.
33 M. Bendahan, R. Boulmani, J. L. Seguin and K. Aguir, *Sens. Actuators, B*, 2004, **100**, 320–324.
34 L. C. Simoes and M. Simoes, *RSC Adv.*, 2013, **3**, 2520–2533.
35 W. H. Glaze, *Environ. Sci. Technol.*, 1987, **21**, 224–230.
36 B. Clavo, D. Ceballos, D. Gutierrez, G. Rovira, G. Suarez, L. Lopez, B. Pinar, A. Cabezon, V. Morales, E. Oliva, D. Fiuza and N. Santana-Rodriguez, *J. Pain Symptom Manage.*, 2013, **46**, 106–112.
37 V. Bocci, I. Zanardi and V. Travagli, *Am. J. Cardiovasc. Drugs*, 2011, **11**, 73–82.
38 D. M. Graham, C. D. Sopher, R. G. Rice and A. E. Yousef, *Food Tech.*, 2013, **67**, 83–84.

39 S. Patil, P. Bourke, J. M. Frias, B. K. Tiwari and P. J. Cullen, *Innovative Food Sci. Emerging Technol.*, 2009, **10**, 551–557.
40 H. P. Kaiser, O. Koster, M. Gresch, P. M. J. Perisset, P. Jaggi, E. Salhi and U. von Gunten, *Ozone: Sci. Eng.*, 2013, **35**, 168–185.
41 C. Y. Wang, R. W. Becker, T. Passow, W. Pletschen, K. Köhler, V. Cimalla and O. Ambacher, *Sens. Actuators, B*, 2011, **152**, 235–240.
42 I. Bilecka and M. Niederberger, *Nanoscale*, 2010, **2**, 1358–1374.
43 M. Baghbanzadeh, L. Carbone, P. D. Cozzoli and C. O. Kappe, *Angew. Chem., Int. Ed.*, 2011, **50**, 11312–11359.
44 M. L. Moreira, G. P. Mambrini, D. P. Volanti, E. R. Leite, M. O. Orlandi, P. S. Pizani, V. R. Mastelaro, C. O. Paiva-Santos, E. Longo and J. A. Varela, *Chem. Mater.*, 2008, **20**, 5381–5387.
45 L. F. da Silva, W. Avansi, J. Andres, C. Ribeiro, M. L. Moreira, E. Longo and V. R. Mastelaro, *Phys. Chem. Chem. Phys.*, 2013, **15**, 12386–12393.
46 G. A. Tompsett, W. C. Conner and K. S. Yngvesson, *ChemPhysChem*, 2006, **7**, 296–319.